IIETA International Information and Engineering Technology Association
Advancing the World of Information and Engineering

Annales de Chimie - Science des Matériaux
Vol. 46, No. 6, December, 2022, pp. 295-299
Journal homepage: http://iieta.org/journals/acsm

Addition Effects of MgO on Structure and Physical Properties in Bi-2212 Ceramics

Nadira Kalkoul[1*], Nora Boussouf[2,3], Saadia Mahjoub[1], Hadda Sahraoui[2,3], Mohamed Fayçal Mosbah[1,4], Sevgi Polat Altintas[5], Nevin Soylu Koc[5]

[1] Material Sciences and Applications Research Unit, Physics Department, Constantine 1 University, B.P. 325 Route d'Ain El Bey, Constantine 25017, Algeria
[2] University Centre of Mila Abdalhafid Boussouf, BP 26 RP, Mila 43000, Algeria
[3] Sciences des Matériaux et Procédés d'Applications, Mila 43000, Algeria
[4] Ecole Nationale Polytechnique de Constantine, Ville Universitaire, Nouvelle Ville Ali Mendjeli, BP : 67A, Algeria
[5] Faculty of Arts and Sciences, Department of Physics, Abant Izzet Baysal University, 14280 Bolu, Turkey

Corresponding Author Email: nkalkoul@yahoo.fr

https://doi.org/10.18280/acsm.460602

Received: 19 October 2022
Accepted: 6 November 2022

Keywords:
MgO addition, Bi-2212 superconductor; superconductivity, X-ray diffraction, critical temperature

ABSTRACT

The effect of magnesium on the microstructural and superconducting characteristics of bulk $Bi_2Sr_2CaCu_2Mg_xO_y$ superconductors with x=0 to 0.05 by solid reaction has been examined in this study. $Bi_2Sr_2CaCu_2O_{8+\delta}$ is formed as the primary phase, and $Bi_2Sr_2CuO_{6+\delta}$ (Bi-2201) is present as the parasitic phase, according to XRD data. In doped samples, the c lattice parameter decreases, indicating that Mg has entered the $Bi_2Sr_2CaCu_2O_{8+\delta}$ crystallographic unit cell. The grain morphology of the samples containing magnesium has changed significantly, and the lamellar structure typical of high temperature superconductors can be seen in the SEM micrographs. The critical temperatures, T_{coff} and T_{conset}, are raised by the addition of Mg, delimiting the superconductive transition. $T_{conset's}$ maximum value corresponds to x = 0.05.

1. INTRODUCTION

The most known and studied bismuth-based high temperature superconductor (HTS) has a general chemical formula $Bi_2Sr_2Ca_{n-1}Cu_nO_{2n+4+\delta}$. Here, n refers to the number of CuO_2 layer in their crystallographic unit cell. The corresponding phases are for n=1: $Bi_2Sr_2CuO_{6+\delta}$; for n=2: $Bi_2Sr_2CaCu_2O_{8+\delta}$ for n=3: $Bi_2Sr_2Ca_2Cu_3O_{10+\delta}$ [1, 2]. For $n \leq 3$, the number n of CuO_2 layers seems to correlates with the value of Tc (R=0) [3]. The Bi-2212 phase is the one among the stated phases that is best suited for its chemical stability and versatility in manufacturing and processing [4]. However, there is the issue of weak links, which could result from inherent flaws in the lattice structure. Possibilities for improving the superconducting properties include filling the pores with the appropriate nanostructures. As in Bi-2223 phase [5, 6], doping with low content of rare earth elementsin the Bi-2212 phase [7-13] changes the normal state properties by decreasing the density of charge carriers n_c (holes) in the CuO_2 planes. In the (n_c, T) plane, n_c defines for the doped compound a phase diagram which limits the conditions for normal, insulating or superconducting state. The transition from insulator to metal state corresponds to thermodynamic fluctuations [14].

Another method that is frequently used to improve the Bi-2212 phase is doping with metallic elements such as B, Na, Zn, and Mg [15-21]. Utilizing MgO particles has a special impact on critical current density and flux pinning among them. Flux pinning, critical current density, and the irreversibility field are all increased in Bi-2212 powders treated with partial-melt processing when 11 and 20 molar percentages of MgO are added [18]. Except for MgO at a concentration of 10 wt%, embedding Bi-2212 single crystals with 1, 5, and 10 wt% enhances the critical current density at low temperatures (20 K) and a maximum applied field of 10 T. Bi-2212 that has been dissolved in an organic solvent and dip-coated on oxidized Ni tapes can have up to 6 vol% MgO added to it to increase the critical current density, up to a maximum of 4 vol% [20]. When 5 weight percent of nanosized MgO particles are added to a single crystal of Bi-2212, the critical current density similarly rises [21]. According to these findings, MgO particles solely serve as pinning centers and lower concentrations produce the best results. Our goal is to investigate the effects of a modest MgO nanoparticle loading (5wt%) on the superconducting characteristics of the Bi-2212 phase.

2. MATERIALS AND METHODS

$Bi_2Sr_2CaCu_2O_{8+\delta}$ phase samples were created using the solid-state reaction technique. The various powders, including Bi_2O_3, $SrCO_3$, $CaCO_3$, and CuO, are combined in the proportion Bi: Sr: Ca: Cu = 2: 2: 1: 2, and the resulting combination is then processed to create a homogeneous powder. For a consistent distribution of the employed products throughout the preparation of our samples, grinding will be done numerous times. After that, the samples will be calcined in air for 30 hours at 810°C. Following calcination, our materials will be again ground and then repeatedly compressed with a hydrostatic press to create cylindrical pellets at a pressure of 5 tons per square centimeter. Our samples were sintered for 60

hours at 840 °C. The subsequent step involves grinding, mixing, and re-pelletizing the obtained pellets with the nominal composition $Bi_2Sr_2CaCu_2Mg_xO_{8+\delta}$ where (x=0, 0.01, 0.02, 0.03, 0.04 and 0.05) in order to improve the grain connectivity and boost the kinetics of the formation of Bi2212 at a second sintering at 850°C for 60 hours.

By using X-ray powder diffraction (XRD) at room temperature (25C), with CuK_α radiation and a step of 0.021°, samples' phase identification was analyzed. XRD pattern indexation and sample cell characteristics were improved using JANA06 software [22]. The energy dispersive X-ray spectrometer (EDS), which is equipped with the scanning electron microscope (SEM), is used to measure the microstructural characteristics. The usual four-probe method was used to measure electrical resistivity, while AC susceptibility was used to measure superconductivity.

3. RESULTS AND DISCUSSION

Figure 1a displays the X-ray diffraction patterns. The majority of the principal diffraction peaks can be attributed to the Bi-2212 phase, according to identification. The parasitic phase Bi-2201 can be recognized by a very low intensity peak at 29.8° denoted by the symbol. Except for x = 0.04, 0.05, where it grows once more, this peak, which was there for x = 0, becomes extremely modest when Mg is added. Secondary phases may be related to the method used, the use of heat treatment, or stoichiometry error [9]. The peaks that correspond to MgO are difficult to identify due to the little addition. The primary peaks (008), (0010), and (0012) have substantially higher intensities than the other three, showing that the grains prefer to be oriented along the (00l) direction.

Figure 1b shows the example diagrams that were calculated and observed. The results of the cell parameter and cell volume refinements are shown in Table 1 for the various samples. The agreement factors R_p, R_{wp}, and the goodness of fit (GOF) factor are also mentioned. Orthorhombic system is present in the polycrystalline phase. The characteristics of the c cell drop from 30.953 Å to 30.782 Å. Although the addition of Mg has no impact on crystal symmetry, the observed drop in c parameter could be explained by Mg^{2+} replacing Ca^{2+}. Mg^{2+} in coordinence 8 has an ionic radius that is 0.89 Å smaller than Ca^{2+}s, which is 1.12 Å [23].

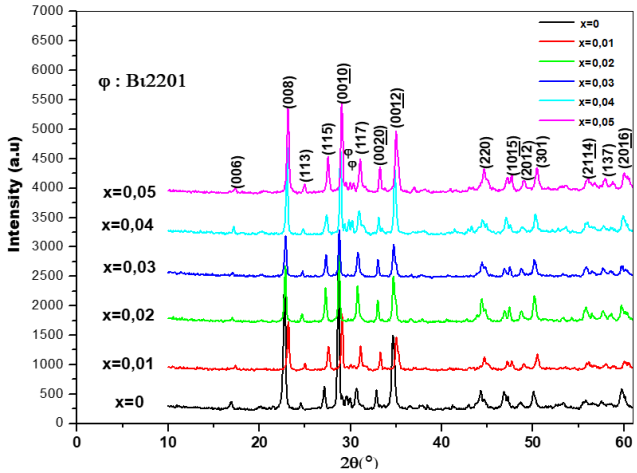

Figure 1a. XRD patterns of $Bi_2Sr_2CaCu_2Mg_xO_{8+\delta}$ samples (x =0 - 0.05)

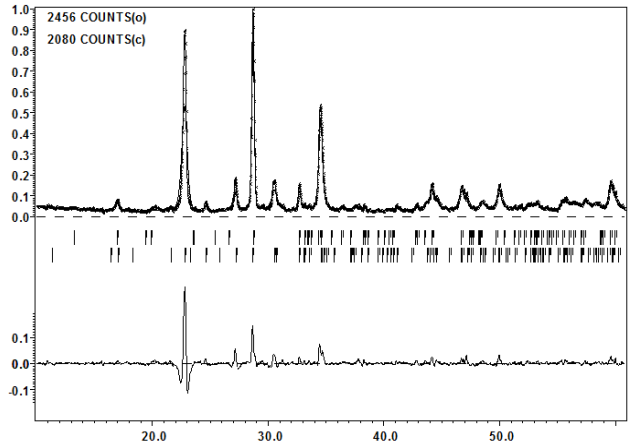

Figure 1b. Observed and calculated XRD patterns for x = 0

Table 1. Lattice parameters (a, b, c), cell volume V, expected weighted profile factor (R_{exp}), weighted profile factor (R_{wp}) and goodness of fit (GOF) of the samples

x	0	0.01	0.02	0.03	0.04	0.05
a(Å)	5.372	5.4153	5. 405	5. 410	5.378	5.384
b(Å)	5.423	5.39599	5.397	5.379	5.415	5.397
c(Å)	30.953	30.8988	30.937	30.936	30.872	30.782
V(Å^3)	901.872	902.8982	902.742	900.477	899.298	894.591
(R_p, R_{wp}) %	(8.70, 13.04)	(6.53, 9.96)	(6.04, 8.92)	(9.35, 12.52)	(10.03, 14.57)	(6.76, 9.41)
GOF	1.70	1.10	0.98	1.21	1.41	1.20

The introduction of MgO also affects the characteristics of a and b cells, with the first one growing and the latter one decreasing. The length of these axes is determined by the length of the Cu-O bond. Additionally, uniform strain would only cause the lattice to expand or contract uniformly, shifting the lattice parameters.

Even though the crystal's symmetry does not change, a very small amount of Bi^{3+} can be replaced with Mg^{2+} and still cause an increase in an axis. The latter reduces the hole concentration and weakens the Cu-O bond [5] due to the shift in how charges are transferred from the charge reservoir (BiO) to the CuO_2 conducting planes. The non-monotonic fluctuation of the a and b axes versus x may be explained by the solubility of MgO particles in the Bi-2212 phase. MgO particles may become trapped by grain boundaries or structural flaws in the samples rather than decomposing and replacing Mg in the Bi-2212 phase. The vortex pinning is made better by this effect. Figure 2 displays SEM images of the samples' surface morphology at the same magnification (5000), with the exception of the sample with x=0.01 (4500). High temperature superconductors have grains with lamellar structures that have uneven block structures. When Mg is supplied with 0.04, grain size, which is greater than 10 m in the undoped sample, drops while porosity rises.

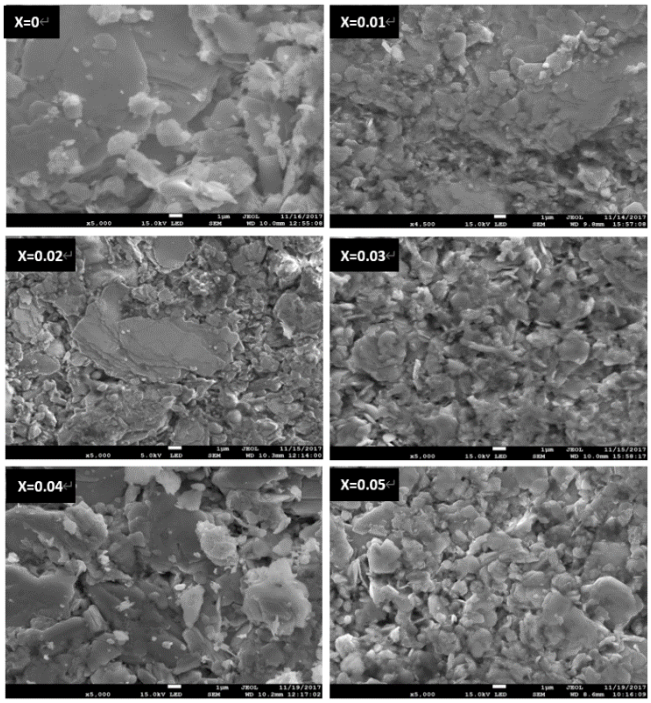

Figure 2. SEM micrographs of the samples with formula: $Bi_2Sr_2CaCu_2Mg_xO_{8+\delta}$ (x=0-0.05)

The samples contain the components of the Bi-2212 phase, as shown by the EDS analysis patterns in Figure 3. All samples with doping contain magnesium. In doped samples, Cu is lower than the value (14.3%) predicted by the stoichiometric formula for Bi-2212, as seen in Table 2.

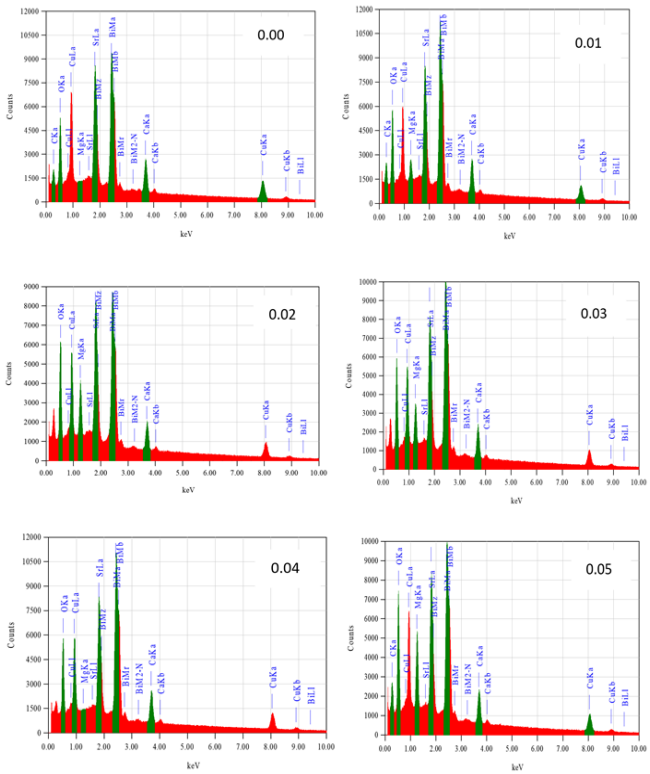

Figure 3. The EDS analysis patterns

Table 2. EDS analyzed composition wt% of the samples

Atom \ x	0.00	0.01	0.02	0.03	0.04	0.05
Bi	40.79	43.42	51.68	55.60	60.29	37.84
Sr	14.58	12.73	18.66	17.77	16.65	12.25
Cu	18.21	12.46	5.16	4.52	4.84	12.54
Ca	4.19	3.85	4.14	4.63	5.05	3.03
Mg	0.01	1.05	3.43	2.46	0.04	3.17
O	11.15	11.60	16.94	15.02	13.13	15.20
C	11.06	14.89	/	/	/	15.98

This outcome raises the option of replacing Cu with Mg, whose composition is substantially higher than anticipated. This fact may be explained by the small detection surface and the small number of grains examined, although an uneven distribution of Mg particles is more likely.

The color map areal distribution of Bi, Sr, Ca, Mg, Ca, Cu, and O was displayed in Figure 4. It is obvious that Mg element aggregation and dispersion throughout Bi2212 grains. The maps of the doped Bi2212 sample with x=0.02 demonstrated the uneven dispersion of Mg oxide (Figure 5). The temperature dependency of the samples' resistivity (T) is shown in Figure 6. The normal state resistivity is discovered to exhibit strong linearity, drop for $1 \leq x \leq 3$ and increase for $x \geq 4$, with the exception of the undoped one. The flaws, grain boundaries, and voids may be to blame for this outcome. The values of the superconducting parameters are shown in Table 3. The $T_{c,onset}$ is increased by the addition of Mg. The Tc is influenced by the connection of the CuO_2 planes as well as their density of charge carriers. This coupling depends on the c-axis value, which is the distance. The density of charge carriers in the sample's normal condition affects the residual resistivity as well. The values reported in Table 3 show that the variation of $T_{c,onset}$ is not related to the density of charge carriers. The situation is the same for the values of $T_{c,off}$. Comparing the variation of the c-axis parameter to the $T_{c,onset}$ one, the correlation is more evident. Moreover, these results confirm the possibility of Mg substituting on Ca site. The behavior of $T_{c,off}$ cannot be correlated to the coupling of the CuO_2 planes because it is more related to the thermal activation of flux n creep. The latter relates to structural defects in the grains of the samples [5]. The large transition width, ΔTc, demonstrated by non-doped sample revealed the individual superconducting grain's inhomogeneities which was showed in the SEM image.

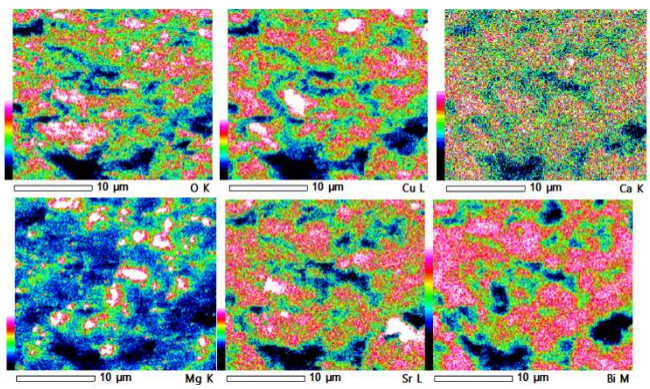

Figure 4. Elemental mapping of sample $Bi_2Sr_2CaCu_2Mg_{0.02}O_{8+\delta}$

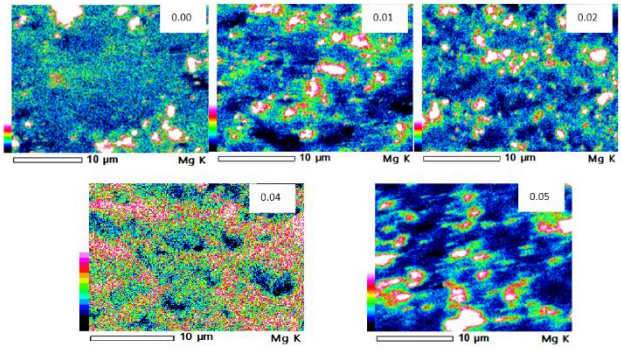

Figure 5. Mapping of Mg in the doped samples

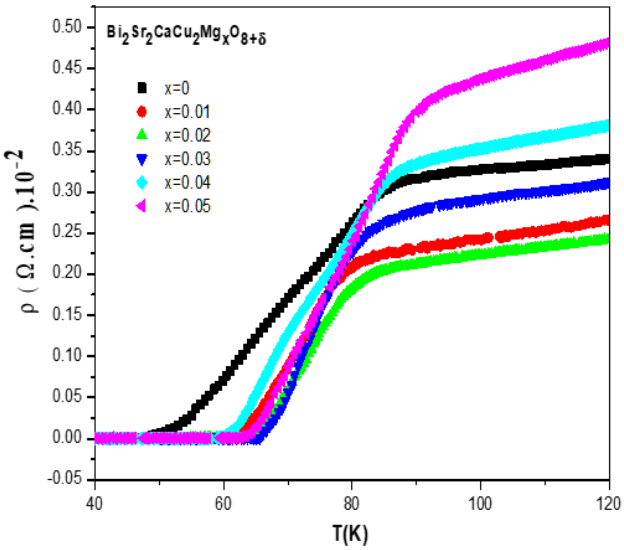

Figure 6. Temperature dependence of resistivity of the $Bi_2Sr_2CaCu_2Mg_xO_{8+\delta}$ samples

Table 3. Critical temperatures, transition width ΔT_c, residual resistivity ρ_0 with different doping

x	0	0.01	0.02	0.03	0.04	0.05
$Tc,_{onset}(K)$	85.7	82	80.7	81	85.6	90.1
$Tc,_{off}$ (K)	52.4	64.3	66.2	67.8	62.8	66.1
$\Delta Tc(K)$	33.3	17.7	14.5	14.3	22.8	24
ρ_0 (Ω. cm) $\times 10^{-3}$	2.87	1.8	1.5	2.1	2.5	2.9

Figure 7 reports the variation of the magnetic susceptibility $\chi(T)$ measured between 10 to 150 K. These results confirm those obtained from resistivity. The decoupling of the grains occurs at a temperature lower than 20 K. This effect confirmed by the absence of the peak in the imaginary part (χ'') is a consequence of the porosity, bad connectivity and extended defects in the samples. Deduced from susceptibility, *Tc* of the doped samples is higher than the undoped one but its variation is not correlate well with the resistivity. The curve of low temperature of χ' indicates that the volume superconducting portion does not shift as *Tc*.

Our results show that addition, at low rate, of MgO influences both the structural and superconducting properties of the Bi2212 phase. Several works have studied this kind of addition in the Bi2223 phase at higher ratio of MgO (until 5 wt.%) with a main result of a decrease of Bi2212 as parasitic phase and higher critical current density J_c [24-26].

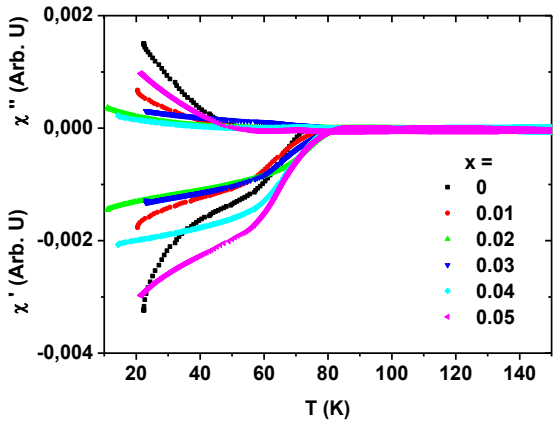

Figure 7. Temperature dependence of the susceptibility χ of the samples with Mg content

Less widely recognized is the possibility of these oxides decomposing and being replaced by Bi2212 in the unit cell as a result. The cell parameters changing supports that theory. The preparation conditions and sintering temperature may be used to explain the non monotonic change. The effect of the addition of metallic oxides may also be explained by the Fermi surface's dependence on doping [27].

4. CONCLUSIONS

The effects of MgO addition on $Bi_2Sr_2CaCu_2O_{8+\delta}$'s micro structural, transport, and magnetic characteristics are discussed in this work. The creation of the Bi2212 phase was demonstrated through analysis of the X-ray diffraction patterns. According to SEM data, porosity is significant in the samples, although it is diminished in the sample with x = 0.05. *Tc* is improved by MgO addition. The structural analysis in conjunction with the results of the resistivity and magnetic experiments appear to support the idea that Mg has been substituted for Cu. With a reduction in the c-axis parameter, there is little change in the samples' crystallographic structure, and the unit cell stays orthorhombic.

REFERENCES

[1] Maeda, H., Tanaka, Y., Fukutomi, M., Asano, T.A. (1988). A new high-T_c oxide superconductor without a rare earth element. Japanese Journal of Applied Physics, 27(2): L209-L210. https://dx.doi.org/10.1143/JJAP.27.L209

[2] Muralidhar, M., Satyavathi, S., Babu, V.H., Pena, O., Sergent, M. (1993). Effect of Ca_2PbO_4 on the formation of the (2223) phase in the Bi-Pb-Sr-Ca-Cu-O system. Materials Science and Engineering: B, 20(3): 312-317. https://doi.org/10.1016/0921-5107(93)90246-J

[3] Chu, W.C., Bechtold, J., Gao, L., Hor, H.P., Huang, J.Z. (1988). Meng, L.R., Sun, Y.Y., Wang, Y.Q., Zue, Y.Y.: Superconductivity up to 114 K in the Bi-Al-Ca-Sr-Cu-O compound system without rare-earth elements. Phys. Rev. Lett. 60(10): 941-943. https://doi.org/10.1103/PhysRevLett.60.941

[4] Zhao, B., Song, W.H., Du, J.J., Sun, Y.P. (2003). Study on resistivity anisotropy and flux pinning of $Bi_{2-x}Pb_xSr_2CaCu_2O_y$ single crystals. Physica C:

Superconductivity, 386: 60-64. https://doi.org/10.1016/S0921-4534(02)02146-9

[5] Hashim, A,. Mamat, R., Kasim, A., Ibrahim, N.S., Mahmud, N.A.C., Rosli, M.M. (2015). Characterization of Dy-doped at Ca site in low-density $Bi_{1.6}Pb_{0.4}Sr_2Ca_{2-x}Dy_xCu_3O_Y$ superconductor. Mal. J. of Anal. Sci., 19(4): 852-859

[6] Bilgili, O., Kocabaş, K. (2015). Effects of Gd substitution on magnetic, structural and superconducting properties of $Bi_{1.7-x}Pb_{0.3}Gd_xSr_2Ca_2Cu_3Oy$. J Mater. Sci.: Mater. Electron, 26(3): 1700-1708.

[7] Meltzow, A.C., Altmeyer, S., Kurz, H., Zakharov, N.D., Senz, S., Hesse, D. (1998). On the influence of rare earth doping on microstructure and phase composition of sputtered, epitaxial $Bi_2Sr_2(Ca_{x-1}Re_x)Cu_2O_{8+\delta}$ films and multilayers. Physica C, 302(2-3): 207-214.

[8] Sun, X.F., Zhao, X., Li, X.G., Ku, H.C. (1999). Hole filling and interlayer coupling in $Bi_2Sr_2Ca_{1-x}Pr_xCu_2O_y$ single crystals. Phys. Rev. B., 59(13): 8978-8993.

[9] Prabitha, V.G., Biju, A., Kumar, A.R.G., Sarun, P.M., Aloysius, R.P., Syamaprasad, U. (2005). Effect of Sm addition on (Bi,Pb)-2212 superconductor. Physica C: Superconductivity, 433(1-2): 28-36. https://doi.org/10.1016/j.physc.2005.09.011

[10] Biju, A., Syamaprasad, U., Rao, A., Xu, J.G., Sivakumar, K.M., Kuo, Y.K. (2007). Structural and transport properties of Nd doped (Bi,Pb)-2212. Physica C: Superconductivity, 466(1-2): 69-75. https://doi.org/10.1016/j.physc.2007.06.013

[11] Vinu, S., Sarun, P.M., Biju, A., Shabna, R., Guruswamy, P., Syamaprasad, U. (2008). The effect of substitution of Eu on the critical current density and flux pinning properties of (Bi,Pb)-2212 superconductor. Supercond. Sci. Technol., 21(4): 045001. https://doi.org/10.1088/0953-2048/21/4/045001

[12] Razia, S., Murikoli, S.P., Surendran, V., Upendran, S. (2009). Doping dependent metal to insulator transition in the (Bi, Pb)-2212 system: The evolution of structural and electronic properties with europium substitution. Chin. Phys. B., 18(9): 4000-4007. https://doi.org/10.1088/1674-1056/18/9/064

[13] Zhang, S., Li, C., Hao, Q., Lu, T., Zhang, P. (2015). Influences of Yb substitution on the intergrain connections and flux pinning properties of Bi-2212 superconductors. Physica C: Superconductivity, 511: 26-32. https://doi.org/10.1016/j.physc.2015.02.004

[14] Storey, J.G., Tallon, J.L., Williams, G.V.M. (2008). Pseudogap ground state in high-temperature superconductors. Phys. Rev. B., 78(14): 1-4. https://doi.org/10.1103/PhysRevB.78.140506

[15] Pignon, B., Autret-Lambert, C., Ruyter, A., Decourt, R., Bassat, J.M., Monot-Laffez, I., Ammor, L. (2008). Study of the yttrium and zinc substitutions effects in $Bi_2Sr_2CaCu_2O_{8+d}$ compounds by transport measurements. Physica C: Superconductivity, 468(11-12): 865-871. https://doi.org/10.1016/j.physc.2007.09.014

[16] Ozkurt, B. (2013). Enhancement in superconducting transition temperature and J_c values in Na-doped $Bi_2Sr_2Ca_1Cu_{2-x}Na_xO_y$ superconductors. J. Mat. Sci.: Mater. Electron, 24(7): 2426-2431. https://doi.org/10.1007/s10854-013-1113-6

[17] Boussouf, N., Mosbah, M.F. (2013). Effects of BCO_3 addition on the formation and properties of the Bi-based superconductors. J. Supercond. Nov. Magn., 26(1): 2891-2897. https://doi.org/10.1007/s10948-012-2091-2

[18] Wei, W., Schwartz, J., Goretta, K.C., Balachandran, U., Bhargava, A. (1998). Effects of nanosize MgO additions to bulk $Bi_{2.1}Sr_{1.7}CaCu_2O_x$. Physica C: Superconductivity, 298(3-4): 279-288. https://doi.org/10.1016/S0921-4534(97)01889-3

[19] Zhao, B., Song, W.H., Wu, X.C., Du, J.J., Sun, Y.P., Wen, H.H., Zhao, Z.X. (2001): Influence of MgO particle doping on flux pinning in $Bi_2Sr_2CaCu_2O_y$ crystals. Physica C: Superconductivity, 361(3): 283-291.

[20] Ni, B., Asayama, K., Kiyuna. S. (2002): Relationship between MgO particles addition and critical current density in Bi2212 thick film grown on oxidized Ni substrate. Physica C., 372-376(3): 1868-1871.

[21] Sasakura, H., Miura, O., Ito, D. (1999). Flux pinning properties in $Bi_2Sr_2CaCu_20_y$ single crystals and the effect of introducing nano-size MgO particles. IEEE Tr. Appl. Supercond, 9(2): 2332-2335. https://doi.org/10.1109/77.784938

[22] Petricek, V., Dusek, M., Palatinus, L. (2006). JANA2006, the Crystallographic Computing System. Praha, Czech Republic, Institute of Physics.

[23] Mihalache, V., Aldica, G., Miu, D. (2006). Modification of the sperconducting parameters of Bi-Sr-Ca-Cu-O by iodine intercalation. Journal of Optoelectronics and Advanced Materials, 8(3): 1287-1291.

[24] Lu, X.Y., Nagata, A., Kamio, D., Sugawara, K., Kamada, S., Watanabe, K., Hanada, S. (2001). Effect of MgO content on the formation and superconducting properties of (Bi,Pb)-2223 phase in the partial-melting and sintering process. Physica C: Superconductivity, 357-360: 828-831. https://doi.org/10.1016/S0921-4534(01)00377-X

[25] Siswayanti, B., Yudanto, S.D., Imaduddin, A., Sebleku, P., Hendrik, N., Lusiana, H., Amal, I., Darsono, N., Amri, F., Syuhada, N., Syahfina, R., Herbirowo, S., Pramono, A.W. (2018). The effect of MgO, CNT, TiO_2 addition on transport properties and formation (Bi,Pb)-2223 prepared by solid state method and recurrent sintering. AIP Conf. Proc., 1964(1): 020039. https://doi.org/10.1063/1.5038321

[26] Lu, X.Y., Yi, D., Chen, H., Nagata, A. (2016): Effect of SnO, MgO and Ag_2O mix-doping on the formation and superconducting properties of Bi-2223 Ag/tapes. Phys. Proc., 81: 129-132. https://doi.org/10.1016/j.phpro.2016.04.020

[27] Drozdov, I.K., Pletikosic, I., Kim, C.K., Fujita, K., Gu, G.D., Davis, S.J.C., Johnson, P.D., Bozovic, I., Valla, T. (2018). Phase diagram of $Bi_2Sr_2CaCu_2O_{8+\delta}$ revisited. Nature Com., 9: 5210.